

# Whispering-gallery-mode emission from biological luminescent protein microcavity assemblies

MATJAŽ HUMAR<sup>1,2,3,5</sup> AND SEOK HYUN YUN<sup>1,4,\*</sup>

<sup>1</sup>Wellman Center for Photomedicine, Harvard Medical School, Massachusetts General Hospital, 65 Landsdowne St. UP-5, Cambridge, Massachusetts 02139, USA

<sup>2</sup>Condensed Matter Department, J. Stefan Institute, Jamova 39, SI-1000 Ljubljana, Slovenia

<sup>3</sup>Faculty of Mathematics and Physics, University of Ljubljana, Jadranska 19, SI-1000 Ljubljana, Slovenia

<sup>4</sup>Harvard-MIT Health Sciences and Technology, Cambridge, 77 Massachusetts Avenue, Cambridge, Massachusetts 02139, USA

<sup>5</sup>e-mail: matjaz.humar@ijs.si

\*Corresponding author: syun@hms.harvard.edu

Received 5 December 2016; revised 11 January 2017; accepted 15 January 2017 (Doc. ID 282124); published 13 February 2017

Fluorescence and bioluminescence are widely used to study biological systems from a molecular to a whole organism level. However, their broadband emission is often a bottleneck for sensitive spectral measurements and multiplexing. To overcome the limitation, the emitters can be coupled with optical cavity modes to generate narrow spectral lines. Here we demonstrate several types of emitter–resonator complexes made of fluorescent or bioluminescent proteins and artificially or naturally formed optical resonators. We engineered cells to express green fluorescent protein (GFP) fused with ABHD5, which binds to oil or lipid droplets supporting whispering gallery modes (WGMs). The genetically integrated complexes feature well-defined WGM spectral peaks. We measured WGM peaks from GFP-coated BaTiO<sub>3</sub> beads (2.56 μm in diameter) during mitosis. Finally, we demonstrate cavity-enhanced bioluminescence using luciferase-coated beads and biochemical excitation. The ability to tailor spontaneous emission via cavity resonance inside biological systems should have applications in biological sensing, imaging, and cell tagging. © 2017 Optical Society of America

**OCIS codes:** (140.3945) Microcavities; (160.1435) Biomaterials; (160.2540) Fluorescent and luminescent materials; (170.1530) Cell analysis; (260.1560) Chemiluminescence.

<https://doi.org/10.1364/OPTICA.4.000222>

## 1. INTRODUCTION

Lasers are widely used for biomedical applications, providing photons for sensing and imaging and delivering optical energy for photothermal and photochemical effects. While the lasers today are built on inanimate engineered materials, and mostly in macroscopic sizes, efforts have recently begun to redesign lasers with biocompatible materials and microscopic scales so that they are more seamlessly integrated with biological systems. At the heart of this new initiative is a biological laser in which all three basic elements of the laser—namely, gain medium, resonator, and pump energy—are provided by biological systems themselves. One of the first steps in this endeavor was the demonstration of protein lasers, where fluorescent proteins in cells allowed lasing [1–4] and optical amplification [5,6]. The genetically produced gain medium provides a means to connect the optical properties of the laser with the genetic and functional phenotypes of the host cell. All the previous protein lasers, however, used external resonators, such as mirrors, placed outside cells. Another major advance in the quest for biological lasers was the recent demonstration of intracellular lasers, made possible by using micrometer-sized spheres made of organic polymers or oil droplets, in

conjunction with organic dyes, as the gain materials [7–9]. Besides the unique characteristics of lasing and stimulated emission, the coupling of the luminescent molecules with optical resonators can alter spontaneous emission kinetics due to wavelength-dependent changes in the optical density of states. This interaction results in emission characteristics distinctly different from the materials' intrinsic luminescence, even at pumping levels below the lasing threshold. At the resonant wavelengths of the cavity, the emission exhibits multiple narrow spectral lines that are enhanced by the optical resonant modes of the cavity [10]. Because of their small mode volumes and high *Q* factors, whispering-gallery-mode (WGM) cavities are especially efficient in exhibiting cavity-enhanced fluorescence. The effect has been widely studied theoretically and experimentally in solid [11] and droplet [12–14] WGM cavities.

Here, we present steps toward all-biological luminescent material, resonator, and pumping by demonstrating several different embodiments of protein-cavity assemblies capable of generating spontaneous emission with multiple narrow spectral lines. First, we demonstrate recombinant green fluorescent protein (GFP) beads in cells, which exhibit distinct WGM features.

Second, we build a cellular system based on genetically modified adipocytes, which makes both a fluorescent material and a resonator genetically integrated and produced by self-assembly. Finally, we integrate cavity resonance and bioluminescence to realize WGM-modified emission driven by chemical energy, without the need for any external light source for optical pumping.

## 2. RESULTS

### A. GFP-Coated Beads *In Vitro*

We have prepared BaTiO<sub>3</sub> glass beads ( $n = 1.95$ ) coated with GFP. Polydisperse BaTiO<sub>3</sub> beads with a size distribution of 1–40  $\mu\text{m}$  (GL0175B, Mo-Sci) were used. Eukaryotic cells can spontaneously internalize microbeads with diameters up to a considerable fraction of the cell size, via endocytosis, without any measurable decrease in their viability [7–9,15]. We have found that the viability of HeLa cells 24 h after engulfing one or more polystyrene beads ( $>6 \mu\text{m}$ ) was  $98.4\% \pm 0.6\%$ , compared to  $99.4\% \pm 0.2\%$  for cells without beads, and the cells containing the beads underwent normal cell division up to several generations. The beads were washed once with acetone, centrifuged at 5,000 g for 5 min, and redispersed in acetone containing 2% v/v 3-aminopropyltriethoxysilane for 15 min with mixing. The beads were then washed twice with acetone and then washed with water and dried at 120°C for 30 min, after which they were incubated in a 10% solution of glutaraldehyde for 1 h. Then the beads were washed three times with water and redispersed in 27  $\mu\text{M}$  GFP solution in phosphate-buffered saline (PBS; pH 7.4). After mixing for 2 h, the beads were washed five times with PBS

using centrifugation. This protocol produced GFP-coated BaTiO<sub>3</sub> beads. For *in situ* real-time measurement of GFP binding, BaTiO<sub>3</sub> beads after incubation with glutaraldehyde were added into a 14 nM GFP solution prepared by adding 10  $\mu\text{l}$  of 0.27  $\mu\text{M}$  GFP solution in 200  $\mu\text{l}$  medium (PBS), so that the amine-reactive surface of the beads accumulated free-floating GFP molecules over time [Fig. 1(a)].

An inverted microscope setup coupled with pump light sources and a spectrometer was used to study the GFP-coated beads (see Fig. S1 of Supplement 1). For the illumination of the GFP and collection of the fluorescence, a  $100\times$  1.40 NA or  $40\times$  1.25 NA oil immersion objective (Olympus) was used. Either a CW 491 nm laser (Cobolt Dual Calypso) or a 455 nm light-emitting diode (LED) (Thorlabs) with a bandpass filter centered at 469 nm and a FWHM of 35 nm was used. Both light sources produced similar results. The collected light was sent through a dichroic mirror (edge at 500 nm) and split 50:50 to a camera (Luca, Andor) and imaging spectrometer (300 mm focal length, 0.05 nm resolution, Andor).

When pumped by a CW blue light at 455 nm, the GFP molecules on the surface emit fluorescence light, which is coupled evanescently into the WGMs of the cavity. Real-time spectral measurement showed that for the initial period of about 30 s, only broad fluorescence emission was measured, but distinct WGM peaks started to appear as increasingly more dispersed GFP molecules were attached onto the bead's surface [Fig. 1(b)]. After  $\sim 100$  s, both the broad fluorescence and WGM peak intensity began to decrease, presumably as the GFP molecules in the solution and on the bead's surface were photobleached

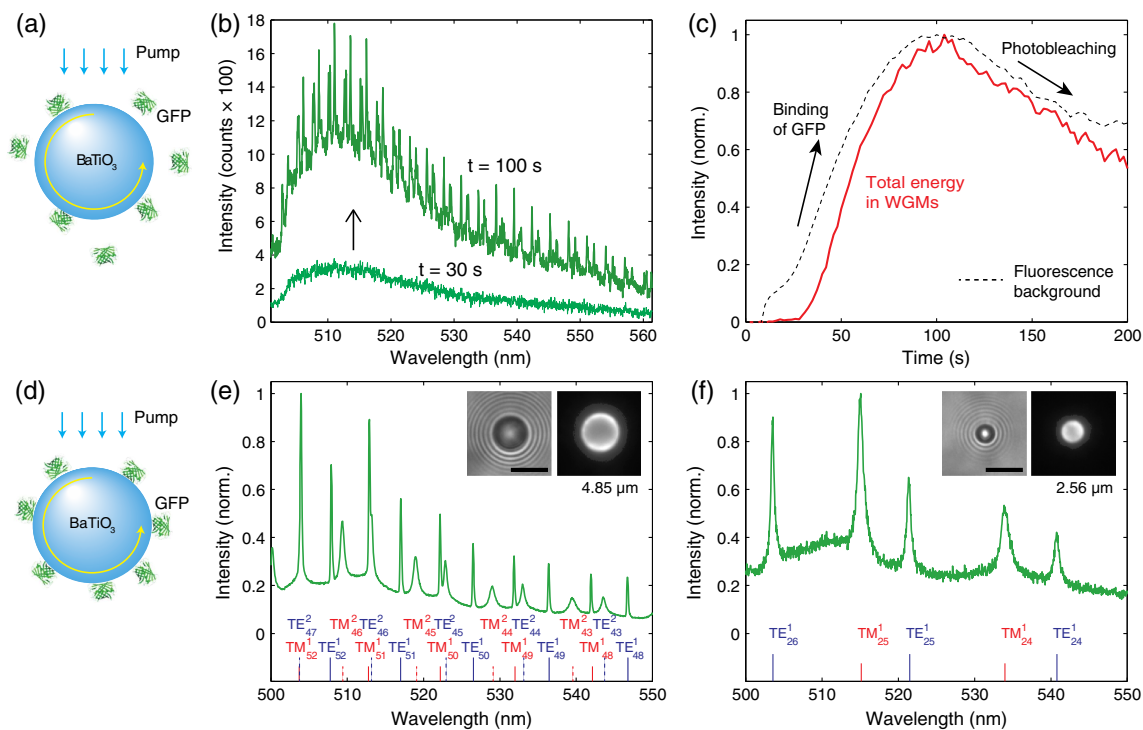


**Fig. 1.** GFP on high-index microspheres. (a) Illustration of GFP molecules binding onto the surface of a BaTiO<sub>3</sub> bead. (b) Fluorescence spectra measured at 30 and 100 s, after adding a GFP solution to beads in dispersion. (c) Intensity of the WGM peaks and background fluorescence after the addition of GFP. (d) A BaTiO<sub>3</sub> glass bead coated with GFP molecules. The fluorescent light from the GFP molecules is coupled into WGMs. (e) Fluorescence spectrum of a BaTiO<sub>3</sub> bead. Curve fitting indicates the oscillation of the first- and second-order radial modes (marked) and predicts a bead diameter of 4.85  $\mu\text{m}$ . Insets show bright-field (left) and fluorescence (right) images of the bead. (f) The output spectrum from a 2.56  $\mu\text{m}$  bead, showing the excitation of only the first-order radial modes. Scale bars, 5  $\mu\text{m}$ .

[Fig. 1(c)]. It should be possible to form GFP layers on internalized beads *in vitro* in GFP-producing cells. This process requires the beads to escape from the endosomes or lysosomes that would trap the beads initially after cellular uptake, so that free-floating GFP in the cytosol interact with the exposed bead's surface.

We analyzed in more detail WGMs in the spectrum emitted by BaTiO<sub>3</sub> glass beads coated with a chemically conjugated monolayer of GFP [Fig. 1(d)]. The output emission showed periodic WGMs on top of a broad fluorescence background. Curve fits [16] indicated the oscillations of the two lowest radial modes with  $Q$  factors as high as 1900 for diameters of 4–5  $\mu\text{m}$  [Fig. 1(e)]. Distinct resonance with a  $Q$  factor of 560 was measured with diameters as small as 2.56  $\mu\text{m}$  [Fig. 1(f)].

For intracellular operation, the GFP-coated BaTiO<sub>3</sub> beads were incubated with and internalized into HeLa cells in culture. HeLa cells (ATCC) were grown at 37°C with 5% CO<sub>2</sub> in full growth medium (Dulbecco's Modified Eagle Medium supplemented with 10% fetal bovine serum and 1% pen-strep), and they were incubated in full growth medium supplied with GFP-coated beads for 12 h prior to optical measurements with pumping by blue LED light. The fluorescence from the cells with intracellular beads exhibited typical WGM spectra (see Fig. S2 of Supplement 1). Cells were viable over a few days, which is the maximum period we have monitored. During this period, we observed cellular division, after which the bead in the parent cell was passed on to one of the two daughter cells [Fig. 2(a)]. We observed dynamic changes in WGM resonance wavelengths, typically by 20–30 pm during cytokinesis [Fig. 2(b)]. This tiny, but measurable, modal shift is due to the change in the bead's surrounding environment, which affects the effective refractive index of the WGMs.

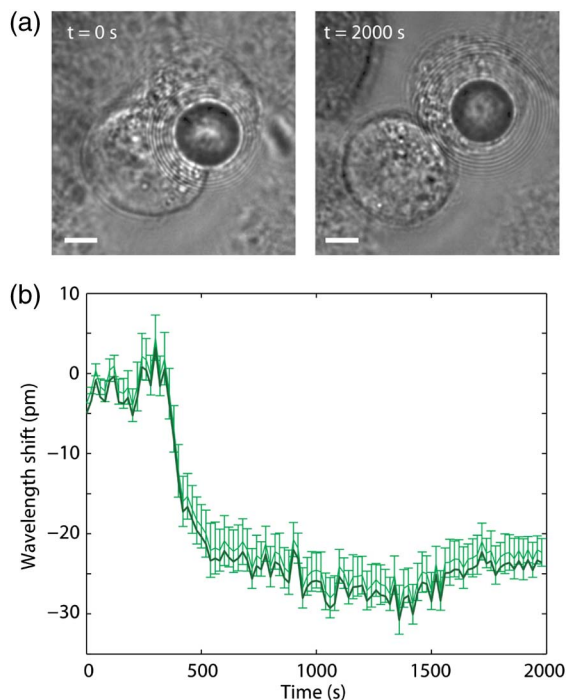


**Fig. 2.** Intracellular GFP-coated glass bead during cell division. (a) Bright-field images showing the transmission of the bead during telophase ( $t = 0$  s) and after cytokinesis ( $t = 2000$  s). Scale bars, 5  $\mu\text{m}$ . (b) Measured spectral shifts of the WGM peaks from telophase to the completion of mitosis.

## B. *In Situ* Assembly of GFP on Injected Oil Droplets

We have previously achieved intracellular lasing by injecting dyed polyphenyl ether (PPE) oil ( $n = 1.69$ ) into the cytosol to form a microdroplet laser [8]. To demonstrate *in vitro* fluorescent material formation, we designed a cellular system based on oil droplets and lipid-binding GFP fusion proteins. We chose  $\alpha/\beta$  hydrolase domain-containing protein 5 (ABHD5), which is known to play roles in intracellular phospholipid metabolism and localize on the surface of lipid droplets [17,18]. For expression of GFP fused to ABHD5 (CGI-58), a plasmid was engineered (pLV[Exp] - EF1A > EGFP::mAbhd5[ORF037106], Cyagen) (see Fig. S3 of Supplement 1). For transduction, the vector was delivered to adipocytes or HeLa cells by HIV-1-derived lentivirus (Cyagen) with a titer concentration of  $(3.31 \pm 2) \times 10^9$  transducing units (TU)/mL, at a multiplicity of infection of 50, with an addition of 8  $\mu\text{g}/\text{ml}$  hexadimethrine bromide (Polybrene, Cyagen), and incubated for 48 h. The cells were washed with fresh medium and incubated for an additional 4 days before the optical measurements. Transduction of HeLa cells with a lentiviral vector encoding the GFP-ABHD5 gene resulted in bright GFP fluorescence with relatively uniform intensity throughout the cytoplasm.

The GFP-transduced HeLa cells were injected with a non-toxic, low-viscosity, high-index PPE oil (SL-5267, Santolubes). The injection was performed using a microinjector (FemtoJet, Eppendorf) and a glass micropipette with a 1.0  $\mu\text{m}$  outer diameter (Femtotip, Eppendorf). The size of the injected droplets was controlled by the injection time, ranging from 0.2 to 1 s, with an injecting pressure of 1700 kPa. The viability of cells 24 h after the injection with PPE, measured using ethidium homodimer-1, was  $82\% \pm 3\%$ , compared to  $99.6\% \pm 0.2\%$  for noninjected cells in the same culture dish. This decrease in viability is probably due to the physical injection. Upon injection of undoped PPE oil using a micropipette [Fig. 3(a)], within less than 1 h an apparent accumulation of GFP on the surface of the droplets was observed under fluorescence microscopy [Fig. 3(b)]. The output spectrum from a single cell when illuminated with a CW laser light (491 nm) showed typical WGM spectral peaks [Fig. 3(c)]. We intentionally photobleached the GFP in the cells [Fig. 3(d)] by extensive exposure to high-intensity CW light for 10 s. Within 6 h after photobleaching, we observed partial, yet significant, recovery of fluorescence brightness both in the cytosol and on the surface of oil droplets [Fig. 3(e)]. This experiment demonstrates the self-healing nature of the genetically integrated, self-assembled fluorescent material.

## C. Self-Assembled Fluorescent Material and Resonator in Adipocyte Cells

To realize both biologically formed fluorescent material and an optical cavity inside a cell, we transduced 3T3-L1 cells, fully differentiated to form large lipid droplets, with a GFP-ABHD5 lentiviral vector [Fig. 4(a)]. 3T3-L1 preadipocytes (ATCC) were grown in glass-bottom 96-well plates at 37°C with 5% CO<sub>2</sub>. The preadipocyte medium (ZenBio) was changed every 2 days until the cells were confluent. Once confluent, the cells were incubated an additional 48 h, after which the medium was exchanged with differentiation medium (ZenBio). After 3 days the medium was replaced by adipocyte maintenance medium (ZenBio), and the medium was exchanged every 3 days for 4 weeks. The adipocytes were then transduced the same way

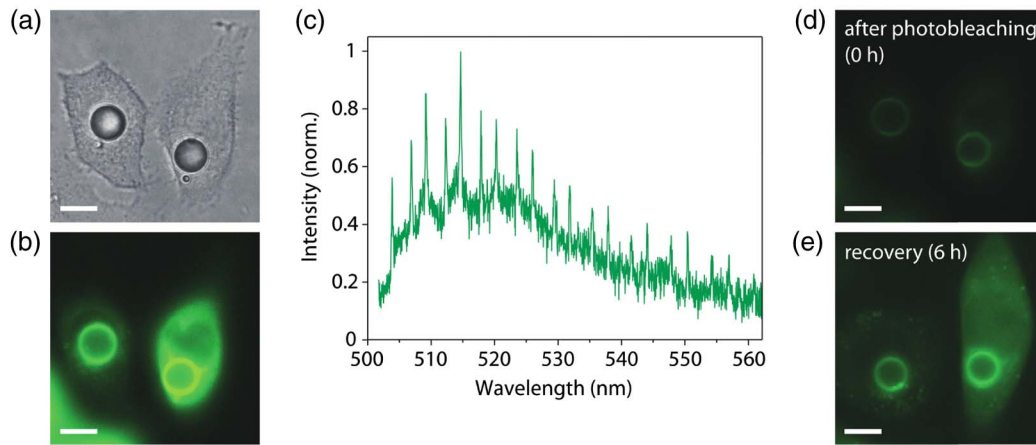


**Fig. 3.** Microcavities in cells with GFP fluorescent material formed *in situ*. (a) Bright-field image of two GFP-ABHD5-producing HeLa cells 2 days after injecting PPE oil droplets into the cytosol. (b) Fluorescence image of the cells, showing bright green fluorescence from the accumulated GFP on the surface of the droplets. (c) Typical output spectrum from the cell under CW pumping. (d) Reduced fluorescence emission after photobleaching by high-intensity optical pumping. (e) Increased fluorescence by continuous production and replenishment of GFP *in vitro* over 6 h after the bleaching. Scale bars, 10  $\mu\text{m}$ .

as the HeLa cells and incubated for an additional 4 days before the optical measurements.

The GFP-ABHD5 fusion protein was found to locate at higher concentrations around the lipid droplets, as was apparent from the bright fluorescent rings [Fig. 4(b)]. The binding mechanism, although not fully understood [19], should involve perilipin, a protein that coats lipid droplets and protects them from lipases. The emission spectrum from a single droplet pumped by CW blue laser light (491 nm) showed a weak, yet well defined, periodic mode structure at a spacing corresponding to the droplet diameter, superimposed on typical broadband GFP fluorescence [Fig. 4(c)]. The WGM peaks were less prominent above the broadband fluorescence because they are wider, with a lower  $Q$  factor. The measured  $Q$  factor was 460, lower than the theoretical radiation-loss-limited  $Q$  factor of 4300 for a droplet of the same size (22  $\mu\text{m}$ ). This discrepancy is reasonable considering the possible unresolvable mode splitting due to droplet deformation [20] and possible scattering loss at contacts with other smaller

lipid droplets in the cytoplasm. In contrast to the GFP-ABHD5-transduced cells, GFP-transduced 3T3-L1 cells showed uniformly dispersed GFP molecules in the cytosol and failed to produce any noticeable cavity-modified spectral features in the fluorescence (see Fig. S4 of Supplement 1).

We illuminated a droplet of a GFP-ABHD5-transduced adipocyte with high-intensity blue laser light (300  $\mu\text{W}$ ) for 200 s to induce bleaching of the GFP, causing a significant reduction in both fluorescence background and WGM structure (see Fig. S5 of Supplement 1). After incubation in the dark for 18 h, the same cell exhibited partial recovery of the fluorescence intensity at the same pumping condition [Fig. 4(d)]. This experiment also demonstrates the remarkable self-healing capability of the biologically formed fluorescent material resonator system.

The  $Q$  factors of intrinsic lipid droplets are not typically sufficient for practical applications in cell tagging and multiplexed imaging, although they may be used for mechanical force sensing via deformation-induced spectral broadening [7]. The size of lipid

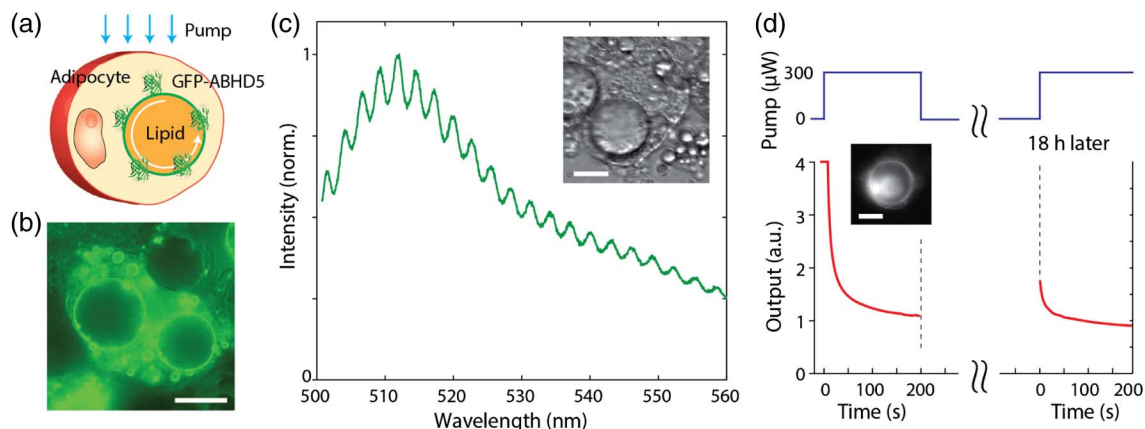


**Fig. 4.** All-biological self-assembled microcavity. (a) Schematic of the intracellular GFP-droplet system. (b) Fluorescence image of GFP-ABHD5-transduced 3T3-L1 mature adipocytes. The fluorescence is mainly emitted from the edges of the droplets. (c) A typical output spectrum from a single GFP-bound lipid droplet (inset). (d) Time-lapse variation of the fluorescence intensity during photobleaching and after partial recovery 18 h later. Inset: fluorescence image at  $t = 0$ . Scale bars, 20  $\mu\text{m}$ .

droplets can change over time as the cells accumulate or consume lipids, possibly enabling precise measurement of adipocyte metabolism.

#### D. Bioluminescence-Pumped WGMs

Bioluminescence produces a photon as a product of a chemical reaction of luciferin, a substrate, and luciferase, an enzyme that catalyses the reaction [21]. To our knowledge, bioluminescence—more generally, chemiluminescence—has not been used before in conjunction with an optical microcavity to generate narrowband spectral peaks. Optically pumped luciferin has been used previously as a fluorescent gain material for WGM lasers [22]. To explore a biochemical-energy-driven light source/resonator system, we used biotinylated *Gaussia* luciferase (GLuc; 19.9 kDa) [23] and conjugated the bioluminescence enzymes onto the streptavidin-coated surface of polystyrene microbeads. SuperAvidin-coated polystyrene microspheres with a mean diameter of 9.95  $\mu\text{m}$  (Bangs Laboratories) were used. The beads were washed twice with Tris buffer (pH 7.8). For conjugation, 2 mg of beads were dispersed in 100  $\mu\text{l}$  of 100  $\mu\text{g/ml}$  biotinylated luciferase and incubated at room temperature for 1 h. GLuc from *Gaussia princeps* (NanoLight) contained biotin covalently attached to the lysine in the AviTag peptide (GLNDIFEAQKIEWHE, C-terminus). This streptavidin–biotin binding system is more effective than nonspecific amine-reactive chemicals, such as glutaraldehyde, which can reduce the activity of luciferase by reacting with the amino groups at the active site [24]. The beads were then washed five times with Tris buffer and transferred to PBS. Bioluminescence was initiated by adding 5  $\mu\text{l}$  of 500  $\mu\text{M}$  water-soluble native coelenterazine (CTZ; Nanolight) in PBS to 100  $\mu\text{g}$  of beads in 95  $\mu\text{l}$  of PBS, producing a final CTZ concentration of

25  $\mu\text{M}$ . For optical measurements, the light source was not used and the dichroic was removed. Instead of a beam splitter a removable mirror was used to direct all the light to either the camera or spectrometer. The spectrometer slit was open to 50  $\mu\text{m}$ , compared to the 15  $\mu\text{m}$  used for fluorescence measurements, to gather more light. The GLuc on the bead's surface oxidizes CTZ(423.46 Da) to generate bioluminescence light, which is evanescently coupled to the WGMs in the bead [Fig. 5(a)]. A single avidin-coated bead has the capacity to bind  $7.9 \times 10^7$  biotinylated luciferase molecules (manufacturer data). Since each luciferase typically produces  $\sim 0.2$  photons/s [25], one bead produces a peak power of  $\sim 1.74 \times 10^6$  photons/s, or 0.72 pW. When we added CTZ (25  $\mu\text{M}$ ) to a medium containing dispersed GLuc-coated beads, a bright bioluminescence emission was generated exclusively from the beads' surfaces [Fig. 5(b)]. The bioluminescence intensity reached the maximum typically in 20–40 s and decayed exponentially (see Fig. S6 of Supplement 1). A representative output spectrum acquired 23 to 28 s after the addition of CTZ shows an easily distinguishable WGM structure [Fig. 5(c)]. Compared to the GFP beads (Fig. 1), the  $Q$  factor and peak-to-background contrast are lower. This is partly due to different spectrometer settings, in which the entrance slit was opened larger (50  $\mu\text{m}$ ) to collect weak bioluminescence more efficiently at the cost of spectral resolution (0.5 nm). A best curve fit to the spectrum predicted an effective bead diameter of 9.378  $\mu\text{m}$ , in reasonable agreement with the manufacturer's specified mean diameter of 9.95  $\mu\text{m}$  [Fig. 4(d)]. Despite the time-dependent variation of the bioluminescence intensity, the spectral fitting of the WGMs yielded accurate measurement of the bead diameter, with a standard deviation error of only  $\pm 1.8$  nm during a 100-s-long measurement [Fig. 5(d)]. Such high precision may

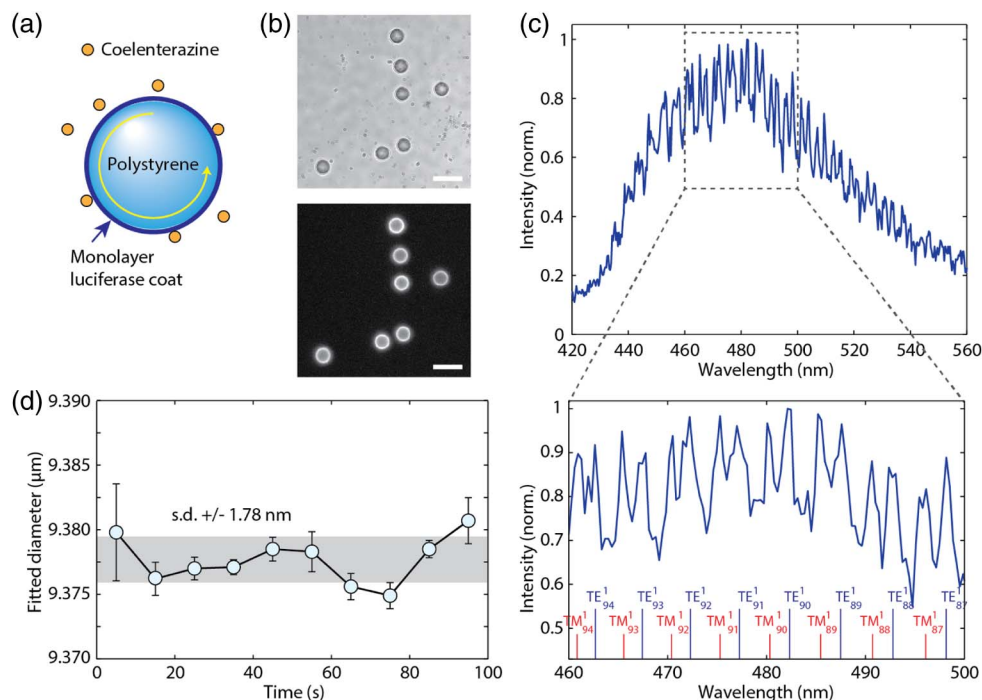


**Fig. 5.** Cavity-modified bioluminescence. (a) Schematic of a polystyrene or glass bead coated with luciferase proteins. Upon addition of luciferin, light is generated and coupled into WGMs. (b) Bright-field image of polystyrene beads coated with luciferase (top) and bioluminescence emission when CTZ is added (bottom). Scale bar, 20  $\mu\text{m}$ . (c) A representative bioluminescence spectrum from a luciferase-coated bead. The spectral peaks of WGMs are fitted to theory to determine the mode orders and bead diameter. (d) The effective bead diameter measured over time. The standard deviation fluctuation (gray area) is  $\sim 190$  ppm.

enable the use of bioluminescence cavity complexes for tagging and sensing in the same way as fluorescent cavities [8], but without the need for an external source of light.

### 3. DISCUSSION AND CONCLUSION

We have demonstrated several schemes to generate cavity-modified luminescence from biological systems by coupling fluorescent proteins and bioluminescence enzymes with microresonators. The building blocks, apart from beads and oils, were genetically integrated and self-assembled in the cytoplasm. The fine spectral features of cavity-tailorable WGMs are suitable for tagging and sensing, adding extra dimension to broadband spectra of fluorescence and bioluminescence. All the demonstrations herein describe spontaneous emission at relatively low pumping levels. Stimulated emission and lasing may be possible with nanosecond optical pumping, a sufficient amount of gain molecules, and a high enough  $Q$  factor, particularly from GFP-accumulated beads [5]. The use of a gain material produced by the cells in the form of fluorescent proteins has several advantages over externally supplied fluorescent dyes. Namely, fluorescent proteins are able to be continuously produced and replenished in the cells, which leads to a unique self-healing capability. Further, only specific cells with certain phenotypes can be chosen to express the gain, so only those cells of interest that generate the desired emission can be studied and tracked. In contrast to the genetically integrated elements, artificial resonators such as glass beads and oil droplets require spontaneous cellular uptake or injection. The GFP-coated BaTiO<sub>3</sub> beads with a diameter of 2.56 μm represent the smallest WGM emitters achieved inside cells. The small size could facilitate the internalization of several beads into a single cell for multiplexed sensing and tagging without substantially disturbing the cell's biological functions. Besides lipid droplets, other types of resonator structures may be devised using various optical [26,27] and plasmonic elements [28] that could be genetically encoded and self-assembled [29,30] inside cells and organisms. The luciferase cavity constructs have the advantages that they do not require external optical pumping, are activated simply by injecting substrate (luciferin) molecules, and have very low background. Moreover, the bioluminescence proteins can be genetically encoded [31] to specific cells. The bioluminescence cavity complexes can be useful for cellular sensing, tagging, and, possibly, photodynamic therapy [32], particularly in tissues at depths not reachable by external optical excitation.

**Funding.** National Institutes of Health (NIH) (P41-EB015903, R01 CA192878, DP1-EB024242); National Science Foundation (NSF) (ECCS-1505569); Human Frontier Science Program (HFSP) (RGP0034/2016); Massachusetts General Hospital (MGH) Research Scholars Award Program; Seventh Framework Programme (FP7) (Marie Curie 627274).

See Supplement 1 for supporting content.

### REFERENCES

- M. C. Gather and S. H. Yun, "Single-cell biological lasers," *Nat. Photonics* **5**, 406–410 (2011).
- M. C. Gather and S. H. Yun, "Lasing from *Escherichia coli* bacteria genetically programmed to express green fluorescent protein," *Opt. Lett.* **36**, 3299–3301 (2011).
- A. Jonas, A. Kiraz, A. Jonáš, M. Aas, Y. Karadag, S. Manioğlu, S. Anand, D. McGloin, H. Bayraktar, and A. Kiraz, "In vitro and in vivo biolasing of fluorescent proteins suspended in liquid microdroplet cavities," *Lab Chip* **14**, 3093–3100 (2014).
- S. Nizamoglu, M. C. Gather, and S. H. Yun, "All-biomaterial laser using vitamin and biopolymers," *Adv. Mater.* **25**, 5943–5947 (2013).
- Q. Chen, M. Ritt, S. Sivaramakrishnan, Y. Sun, and X. Fan, "Optofluidic lasers with a single molecular layer of gain," *Lab Chip* **14**, 4590–4595 (2014).
- M. C. Gather and S. H. Yun, "Bio-optimized energy transfer in densely packed fluorescent protein enables near-maximal luminescence and solid-state lasers," *Nat. Commun.* **5**, 5722 (2014).
- M. Himmelhaus and A. Francois, "In vitro sensing of biomechanical forces in live cells by a whispering gallery mode biosensor," *Biosens. Bioelectron.* **25**, 418–427 (2009).
- M. Humar and S. H. Yun, "Intracellular microlasers," *Nat. Photonics* **9**, 572–576 (2015).
- M. Schubert, A. Steude, P. Liehm, N. M. Kronenberg, M. Karl, E. C. Campbell, S. J. Powis, and M. Gather, "Lasing within live cells containing intracellular optical micro-resonators for barcode-type cell tagging and tracking," *Nano Lett.* **15**, 5647–5652 (2015).
- B. Gayral, "Controlling spontaneous emission dynamics in semiconductor micro cavities," *Ann. Phys.* **26**, 1–135 (2001).
- R. E. Benner, P. W. Barber, J. F. Owen, and R. K. Chang, "Observation of structure resonances in the fluorescence-spectra from microspheres," *Phys. Rev. Lett.* **44**, 475–478 (1980).
- A. J. Campillo, J. D. Eversole, and H.-B. Lin, "Cavity quantum electrodynamic enhancement of stimulated emission in microdroplets," *Phys. Rev. Lett.* **67**, 437–440 (1991).
- S. Holler, N. L. Goddard, and S. Arnold, "Spontaneous emission spectra from microdroplets," *J. Chem. Phys.* **108**, 6545–6547 (1998).
- S. Arnold, "Cavity-enhanced fluorescence decay rates from microdroplets," *J. Chem. Phys.* **106**, 8280–8282 (1997).
- G. J. Cannon and J. A. Swanson, "The macrophage capacity for phagocytosis," *J. Cell Sci.* **101**, 907–913 (1992).
- M. L. Gorodetsky and A. E. Fomin, "Geometrical theory of whispering-gallery modes," *IEEE J. Sel. Top. Quantum Electron.* **12**, 33–39 (2006).
- V. Subramanian, A. Rothenberg, C. Gomez, A. W. Cohen, A. Garcia, S. Bhattacharyya, L. Shapiro, G. Dolios, R. Wang, M. P. Lisanti, D. L. Brasaemle, A. Rotlienber, C. Gomez, A. W. Cohen, A. Garcia, S. Bhattacharyya, L. Shapiro, G. Dolios, R. Wang, M. P. Lisanti, and D. L. Brasaemle, "Perilipin A mediates the reversible binding of CGI-58 to lipid droplets in 3T3-L1 adipocytes," *J. Biol. Chem.* **279**, 42062–42071 (2004).
- T. Yamaguchi, N. Omatsu, S. Matsushita, and T. Osumi, "CGI-58 interacts with perilipin and is localized to lipid droplets, possible involvement of CGI-58 mislocalization in Chanarin-Dorfman syndrome," *J. Biol. Chem.* **279**, 30490–30497 (2004).
- A. R. Thiam, R. V. Farese, Jr., and T. C. Walther, "The biophysics and cell biology of lipid droplets," *Nat. Rev. Mol. Cell Biol.* **14**, 775–786 (2013).
- N. Riesen, T. Reynolds, A. François, M. R. Henderson, and T. M. Monro, "Q-factor limits for far-field detection of whispering gallery modes in active microspheres," *Opt. Express* **23**, 28896–28904 (2015).
- C. H. Contag and M. H. Bachmann, "Advances in in vivo bioluminescence imaging of gene expression," *Annu. Rev. Biomed. Eng.* **4**, 235–260 (2002).
- X. Wu, Q. Chen, Y. Sun, and X. Fan, "Bio-inspired optofluidic lasers with luciferin," *Appl. Phys. Lett.* **102**, 11–13 (2013).
- B. Kay, S. Thai, and V. Volgina, "High-throughput biotinylation of proteins," in *High Throughput Protein Expression and Purification*, S. Doyle, ed., Vol. **498** of *Methods in Molecular Biology* (Humana, 2009), pp. 185–198.
- A. R. Ribeiro, R. M. Santos, L. M. Rosário, and M. H. Gil, "Immobilization of luciferase from a firefly lantern extract on glass strips as an alternative strategy for luminescent detection of ATP," *J. Biolumin. Chemilumin.* **13**, 371–378 (1998).
- A. M. Loening, A. M. Wu, and S. S. Gambhir, "Red-shifted *Renilla reniformis* luciferase variants for imaging in living subjects," *Nat. Methods* **4**, 641–643 (2007).
- M. Humar, S. J. J. Kwok, M. Choi, S. Cho, A. K. Yetisen, and S.-H. Yun, "Towards biomaterial-based implantable photonic devices," *Nanophotonics* **5**, 60–80 (2016).

27. R. M. Kramer, W. J. Crookes-Goodson, and R. R. Naik, "The self-organizing properties of squid reflectin protein," *Nat. Mater.* **6**, 533–538 (2007).
28. J. A. Fan, C. Wu, K. Bao, J. Bao, R. Bardhan, N. J. Halas, V. N. Manoharan, P. Nordlander, G. Shvets, and F. Capasso, "Self-assembled plasmonic nanoparticle clusters," *Science* **328**, 1135–1138 (2010).
29. P. W. K. Rothmund, "Folding DNA to create nanoscale shapes and patterns," *Nature* **440**, 297–302 (2006).
30. W. B. Rogers, W. M. Shih, and V. N. Manoharan, "Using DNA to program the self-assembly of colloidal nanoparticles and microparticles," *Nat. Rev. Mater.* **1**, 16008 (2016).
31. M. P. Hall, J. Unch, B. F. Binkowski, M. P. Valley, B. L. Butler, M. G. Wood, P. Otto, K. Zimmerman, G. Vidugiris, T. MacHleidt, M. B. Robers, H. A. Benink, C. T. Eggers, M. R. Slater, P. L. Meisenheimer, D. H. Klaubert, F. Fan, L. P. Encell, and K. V. Wood, "Engineered luciferase reporter from a deep sea shrimp utilizing a novel imidazopyrazinone substrate," *ACS Chem. Biol.* **7**, 1848–1857 (2012).
32. Y. R. Kim, S. Kim, J. W. Choi, S. Y. Choi, S.-H. Lee, H. Kim, S. K. Hahn, G. Y. Koh, and S. H. Yun, "Bioluminescence-activated deep-tissue photodynamic therapy of cancer," *Theranostics* **5**, 805–817 (2015).